PHYSICAL REVIEW B **84**, 041412(R) (2011)

Multiterminal single-molecule–graphene-nanoribbon junctions with the thermoelectric figure of merit optimized via evanescent mode transport and gate voltage

Kamal K. Saha,[1] Troels Markussen,[2] Kristian S. Thygesen,[2] and Branislav K. Nikolić[1,*]

[1]*Department of Physics and Astronomy, University of Delaware, Newark, Delaware 19716-2570, USA*

[2]*Center for Atomic-scale Materials Design (CAMD), Department of Physics, Technical University of Denmark, DK-2800 Kongens Lyngby, Denmark*

(Received 30 June 2011; published 29 July 2011)

We propose thermoelectric devices where a single molecule is connected to two metallic zigzag graphene nanoribbons (ZGNRs) via highly transparent contacts that allow the injection of evanescent wave functions from ZGNRs. Their overlap generates a peak in the electronic transmission that is largely *insensitive* to the type of the short conjugated molecule, while ZGNRs additionally suppress hole-like contributions to the thermopower. Thus optimized thermopower, together with suppression of phonon transport through a ZGNR-molecule-ZGNR structure, yields the thermoelectric figure of merit $ZT \sim 0.5$ at room temperature and $0.5 < ZT < 2.5$ below liquid nitrogen temperature. Using density functional theory combined with the nonequilibrium Green's function formalism for multiterminal devices, we show how the transmission resonance can be manipulated by the voltage applied to a third ZGNR top-gate electrode covering the molecule to further tune the value of ZT.

DOI: 10.1103/PhysRevB.84.041412 PACS number(s): 85.80.Fi, 72.80.Vp, 73.63.Rt, 81.07.Nb

Thermoelectrics transform temperature gradients into electric voltage and vice versa. Although a plethora of thermoelectric-based energy conversion and cooling applications have been envisioned, their usage is presently limited by their small efficiency.[1] Careful tradeoffs are needed to optimize the dimensionless figure of merit $ZT = S^2GT/\kappa$ quantifying the maximum efficiency of a thermoelectric conversion because ZT contains an unfavorable combination of the thermopower S, average temperature T, electrical conductance G, and total thermal conductance $\kappa = \kappa_{\rm el} + \kappa_{\rm ph}$ (including contributions from electrons $\kappa_{\rm el}$ and phonons $\kappa_{\rm ph}$). The devices with $ZT > 1$ are regarded as good thermoelectrics, but $ZT > 3$ is required for them to compete with conventional generators and refrigerators.[1]

The major experimental efforts to increase ZT have been focused on suppressing the phonon conductivity using either complex (through disorder in the unit cell) bulk materials[2] or bulk nanostructured materials.[3] A complementary approach engineers electronic density of states to obtain a sharp singularity[3] near the Fermi energy which can enhance the power factor S^2G.

Very recent experiments[4] and theoretical studies[5–10] have ignited the exploration of devices where a single molecule is attached to metallic[7] or semiconducting[8] electrodes, so that dimensionality reduction and possible strong electronic correlations[10] make it possible to increase S concurrently with diminishing $\kappa_{\rm ph}$ while keeping the nanodevice disorder-free.[11] For example, creation of sharp transmission resonances near the Fermi energy E_F by tuning the *chemical properties* of the molecule and molecule-electrode contact can substantially enhance the thermopower S which depends on the derivative of the conductance near E_F. At the same time, the presence of a molecule in the electrode-molecule-electrode heterojunction severely disrupts phonon propagation when compared to a homogenous clean electrode.

In this Rapid Communication, we exploit a transparent contact between metallic zigzag graphene nanoribbon (ZGNR) electrodes and a ring-shaped 18-annulene molecule to propose two-terminal (i.e., the top gate is absent in Fig. 1) and three-terminal devices illustrated in Fig. 1. Their thermoelectric properties are analyzed using the nonequilibrium Green's function (NEGF) combined with density functional theory (DFT) formalism[12,13] recently extended[14,15] to multiterminal (MT) nanostructures (the MT-NEGF-DFT framework). The high contact transparency allows evanescent modes from the two ZGNR electrodes to tunnel into the molecular region and meet in the middle of it (when the molecule is short enough[16]), which is a counterpart of the well-known metal-induced gap states in metal-semiconductor Schottky junctions. This effect can induce a large peak (i.e., a resonance) in the electronic transmission function near E_F [Fig. 2(a)], despite the energy difference between the highest occupied molecular

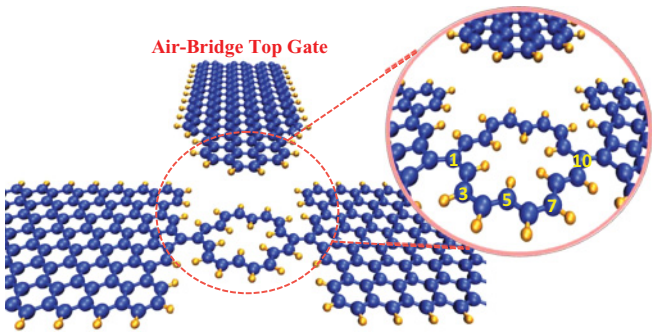

FIG. 1. (Color online) Schematic view of the proposed ZGNR|18-annulene|ZGNR three-terminal heterojunction. The contact between the source and drain 8-ZGNR (consisting of eight zigzag chains) metallic electrodes and a ring-shaped molecule is made via five-membered rings of carbon atoms (dark blue/dark gray), while the electrodes are attached to atoms 1 and 10 of the molecule. The third electrode is coupled as an "air-bridge" top gate, made of ZGNR as well, covering only the molecular ring at the distance 5.3 Å. The two-terminal version of the device assumes that such top gate is absent. The hydrogen atoms (light yellow/light gray) are included to passivate the edge carbon atoms.

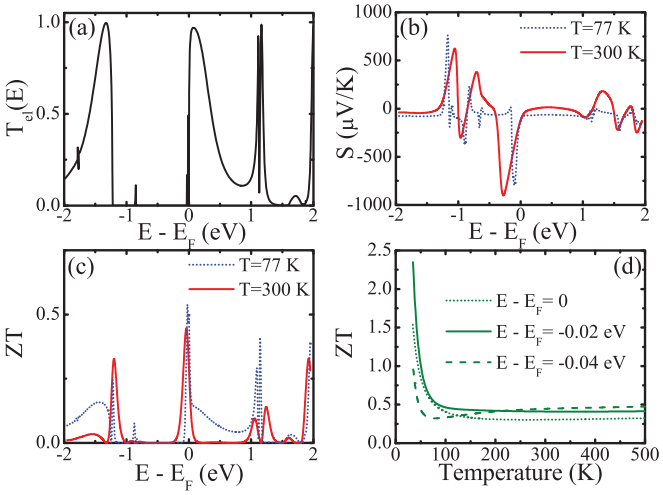

FIG. 2. (Color online) Physical quantities determining thermoelectric properties of the two-terminal device shown in Fig. 1 (without the top-gate electrode): (a) zero-bias electronic transmission $\mathcal{T}_{\rm el}(E)$; (b) the corresponding thermopower S at two different temperatures; (c) thermoelectric figure of merit ZT vs energy at two different temperatures; and (d) ZT vs temperature at three different energies.

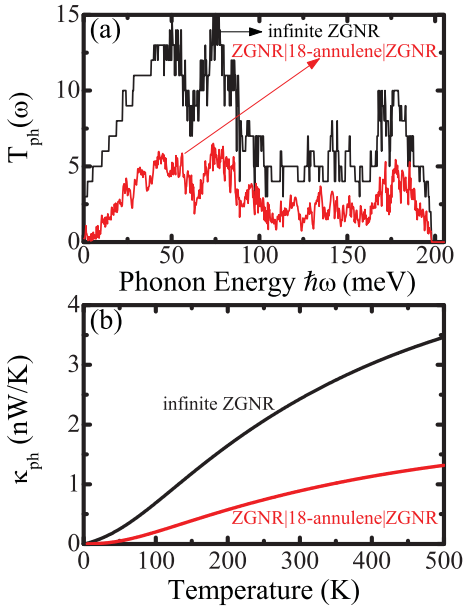

FIG. 3. (Color online) (a) The phonon transmission function $\mathcal{T}_{\rm ph}(\omega)$ and (b) the corresponding thermal conductance $\kappa_{\rm ph}$ for an infinite 8-ZGNR and the two-terminal device shown in Fig. 1 (assuming absence of the third top-gate electrode) whose electrodes are made of semi-infinite 8-ZGNR.

orbital (HOMO) and the lowest unoccupied molecular orbital (LUMO), called the HOMO-LUMO energy gap, of the isolated molecule.

The enhancement of the thermopower [Fig. 2(b)] due to transmission resonance around $E \geqslant E_F$ and suppression of the hole-like contribution (i.e., negligible transmission around $E < E_F$) to S, together with several times smaller phonon thermal conductance (Fig. 3) when compared to infinite ZGNR, yields the maximum room-temperature $ZT \sim 0.5$ in the two-terminal device [Figs. 2(c) and 2(d)]. Furthermore, we discuss how a third top-gate ZGNR electrode covering the molecule, while being separated by an air gap in Fig. 1, can tune the properties of the transmission resonance via the applied gate voltage thereby making possible further enhancement of ZT (Fig. 4).

Among the recent theoretical studies of molecular thermoelectric devices via the NEGF-DFT framework,[7,8] most have been focused[7] on computing the thermopower S, with only a few[8] utilizing DFT to obtain forces on displaced atoms and then compute $\kappa_{\rm ph}$. Moreover, due to the lack of NEGF-DFT algorithms for *multiterminal* nanostructures, the possibility to tune thermoelectric properties of single-molecule devices via the usage of the third electrode has remained largely an unexplored realm.[9] We note that the recent proposal[8] for two-terminal molecular thermoelectric devices with the sophisticated combination of a local chemical tuning of the molecular states and usage of semiconducting electrodes has predicted much smaller $ZT \sim 0.1$ at room temperature. In addition, our $0.5 < ZT < 2.5$ at $E - E_F = -0.02$ eV (which can be set by the back-gate electrode covering the whole device[17]) in the temperature range $T = 30$–77 K is much larger than the value achieved in conventional low-temperature bulk thermoelectric materials.[2]

The recent fabrication of GNRs with ultrasmooth edges,[18] where those with zigzag edges are insulating at very low temperatures due to edge magnetic ordering which is nevertheless easily destroyed[19] above $\gtrsim$10 K, has opened new avenues for highly controllable molecular junctions with a well-defined molecule-electrode contact characterized by high transparency, strong directionality, and reproducibility. This is because the strong molecule-GNR π-π coupling makes possible the formation of a continuous π-bonded network across the GNR and orbitals of conjugated organic molecules.[16] Unlike the metallic carbon nanotubes (CNTs) employed experimentally[20] to generate such networks,[16] GNRs have a planar structure appropriate for aligning and patterning.

The early experiments[20] on CNT|molecule|CNT heterojunctions have measured surprisingly small conductances for a variety of sandwiched molecules. The first-principles analysis of different setups reveals that this is due to significant twisting forces when the molecule is connected to the CNT via, e.g., six-membered rings.[16] Therefore, to keep a nearly parallel and in-plane configuration (hydrogen atoms of 18-annulene slightly deviate from the molecular plane) of our ZGNR|18-annulene|ZGNR junction, we use a five-membered ring[16] in Fig. 1 to chemically bond ZGNR to annulene.

The carbon atoms of a ring-shaped 18-annulene molecule can be connected to ZGNR electrodes in configurations whose Feynman paths for electrons traveling around the ring generate either constructive or destructive quantum interference effects imprinted on the conductance.[21] For example, a π electron at E_F entering the molecule in setup (1,10) shown in Fig. 1 has the wavelength $k_F/2d$ (d is the spacing between carbon atoms within the molecule), so that for the two simplest Feynman paths of length $9d$ (upper half of the ring) and $9d$ (lower half of the ring) the phase difference is 0. Note that the destructive quantum interference[21] would form an additional

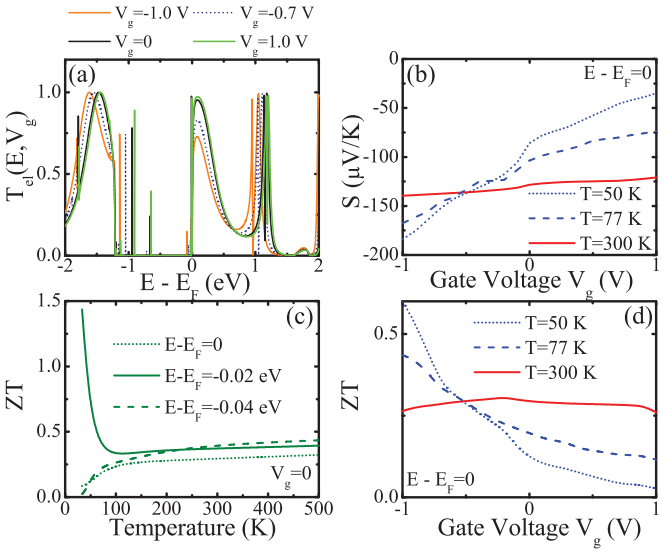

FIG. 4. (Color online) Physical quantities determining thermoelectric properties of the three-terminal device shown in Fig. 1 as a function of the applied gate voltage V_g: (a) zero-bias electronic transmission $\mathcal{T}_{\rm el}(E,V_g)$; (b) the corresponding thermopower S at three different temperatures; (c) ZT vs temperature at $V_g = 0$; and (d) ZT vs V_g at three different temperatures.

dip (i.e., antiresonance) within the main transmission peak in Fig. 2(a) generated by the injection of overlapped evanescent modes.[15] The effect of antiresonance on the thermopower S for gold|18-annulene|gold junctions has been studied in Ref. 22 as a possible sensitive tool to confirm the effects of quantum coherence on transport through single-molecule junctions.

The computation of quantities entering ZT for realistic single-molecule junctions requires quantum transport methods combined with *first-principles* input about atomistic and electronic structure to capture *charge transfer* in equilibrium (which is indispensable to obtaining the correct zero-bias transmission of, e.g., carbon-hydrogen systems[13]), geometrically optimized atomic positions of the molecular bridge including molecule-electrode separation in equilibrium, and forces on atoms when they are perturbed out of equilibrium. The state-of-the-art approach that can capture these effects, as long as the coupling between the molecule and the electrodes is strong enough to ensure transparent contact and diminish Coulomb blockade effects,[10,12] is NEGF-DFT.[12,13]

The technical details of the construction of the nonequilibrium density matrix via NEGF-DFT for multiterminal devices are discussed in Ref. 14. Our MT-NEGF-DFT code utilizes ultrasoft pseudopotentials and Perdew-Burke-Ernzerhof (PBE) parametrization of the generalized gradient approximation for the exchange-correlation functional. The localized basis set for DFT calculations is constructed from atom-centered orbitals (six per C atom and four per H atom) that are optimized variationally for the electrodes and the central molecule separately while their electronic structure is obtained concurrently.

In the coherent transport regime, the NEGF post-processing of the result of the DFT self-consistent loop expresses the zero-bias electron transmission function between the left (L) and the right (R) electrodes as

$$\mathcal{T}_{\rm el}(E) = {\rm Tr}\{\mathbf{\Gamma}_R(E)\mathbf{G}(E)\mathbf{\Gamma}_L(E)\mathbf{G}^\dagger(E)\}. \quad (1)$$

The matrices $\mathbf{\Gamma}_{L,R}(E) = i[\mathbf{\Sigma}_{L,R}(E) - \mathbf{\Sigma}^\dagger_{L,R}(E)]$ account for the level broadening due to the coupling to the electrodes, where $\mathbf{\Sigma}_{L,R}(E)$ are the self-energies introduced by the ZGNR electrodes.[13] The retarded Green's function matrix of the central region (molecule + portion of electrodes) is given by $\mathbf{G} = [E\mathbf{S} - \mathbf{H} - \mathbf{\Sigma}_L - \mathbf{\Sigma}_R]^{-1}$, where in the local orbital basis $\{\phi_i\}$ Hamiltonian matrix $\mathbf{H}$ is composed of elements $H_{ij} = \langle\phi_i|\hat{H}_{\rm KS}|\phi_j\rangle$ ($\hat{H}_{\rm KS}$ is the effective Kohn-Sham Hamiltonian obtained from the DFT self-consistent loop) and the overlap matrix $\mathbf{S}$ has elements $S_{ij} = \langle\phi_i|\phi_j\rangle$.

The transmission function of Eq. (1) obtained within the NEGF-DFT framework allows us to compute the following integrals:[23]

$$K_n(\mu) = \frac{2}{h}\int_{-\infty}^{\infty} dE\, \mathcal{T}_{\rm el}(E)(E-\mu)^n \left(-\frac{\partial f(E,\mu)}{\partial E}\right), \quad (2)$$

where $f(E,\mu) = \{1 + \exp[(E-\mu)/k_BT]\}^{-1}$ is the Fermi-Dirac distribution function at the chemical potential μ. The knowledge of $K_n(\mu)$ finally yields all electronic quantities in the expression for ZT: $G = e^2K_0(\mu)$; $S = K_1(\mu)/[eTK_0(\mu)]$; and $\kappa_{\rm el} = \{K_2(\mu) - [K_1(\mu)]^2/K_0(\mu)\}/T$.

The phonon thermal conductance is obtained from the phonon transmission function $\mathcal{T}_{\rm ph}(\omega)$ using the corresponding Landauer-type formula[5] for the central region attached to two semi-infinite electrodes:

$$\kappa_{\rm ph} = \frac{\hbar^2}{2\pi k_BT^2}\int_0^\infty d\omega\,\omega^2\mathcal{T}_{\rm ph}(\omega)\frac{e^{\hbar\omega/k_BT}}{(e^{\hbar\omega/k_BT}-1)^2}. \quad (3)$$

The phonon transmission function $\mathcal{T}_{\rm ph}(\omega)$ can be calculated from the same Eq. (1) with substitutions $\mathbf{H} \to \mathbf{K}$ and $E\mathbf{S} \to \omega^2\mathbf{M}$, where $\mathbf{K}$ is the force constant matrix and $\mathbf{M}$ is a diagonal matrix with the atomic masses. We obtain the force constant matrix using GPAW, which is a real space electronic structure code based on the projector augmented wave method.[24] The electronic wave functions are expanded in atomic orbitals with a single-ζ polarized basis set, and a PBE exchange-correlation functional is used. The whole central region, which includes 27 layers of ZGNR electrodes, is first relaxed to a maximum force of 0.01 eV/Å per atom. Subsequently, we displace each atom I by $Q_{I\alpha}$ in the direction $\alpha = \{x,y,z\}$ to get the forces $F_{J\beta}(Q_{I\alpha})$ on atom $J \neq I$ in direction β. The elements of $\mathbf{K}$ are then computed from finite differences, $K_{I\alpha,J\beta} = [F_{J\beta}(Q_{I\alpha}) - F_{J\beta}(-Q_{I\alpha})]/2Q_{I\alpha}$. The intra-atomic elements are calculated by imposing momentum conservation, such that $K_{I\alpha,I\beta} = -\Sigma_{J\neq I}K_{I\alpha,J\beta}$.

Figure 2(a) shows the zero-bias electronic transmission $\mathcal{T}_{\rm el}(E)$ for the two-terminal version of the device in Fig. 1, where the peak near E_F is conspicuous. Additionally, the suppression of the hole-like transmission [$\mathcal{T}_{\rm el}(E) \to 0$ around $E < E_F$] evades unfavorable compensation[8] of hole-like and electron-like contributions to the thermopower. This is due to the symmetry of the valence band propagating transverse mode in the GNR semi-infinite electrode which changes sign at the two carbon atoms closest to the molecule for the geometry (molecule connected to the middle of the GNR

edge) in Fig. 1. We emphasize that these features of $\mathcal{T}_{el}(E)$ are *largely insensitive to the details of short conjugated molecules*, as demonstrated by very similar results obtained for the ZGNR|C10|ZGNR heterojunction.[25] Also, since they are governed by the ZGNR Bloch states, they are *impervious* to the usual poor estimates of the band gap size and molecular energy level position in DFT.

The maximum value of the corresponding thermopower S plotted in Fig. 2(b) is slightly away from $E - E_F = 0$ and it is an *order of magnitude larger* than the one measured on large-area graphene[17] or in molecular junctions with gold electrodes.[4] Moreover, the interruption of the infinite ZGNR by a molecule acts unfavorably to phonon transmission $\mathcal{T}_{ph}(\omega)$, thereby generating three times smaller κ_{ph} at room temperature when compared in Fig. 3 to the thermal conductance of an infinite 8-ZGNR. Figures 2(c) and 2(d) demonstrate that the interplay of large S^2G and reduced κ_{ph} for the proposed two-terminal device yields the room-temperature $ZT \sim 0.5$ around $E - E_F = 0$.

The introduction of the narrow air-bridge top-gate electrode in Fig. 1, which is positioned at the distance 5.3 Å (ensuring negligible tunneling leakage current into such third ZGNR electrode) away from the two-terminal device underneath while covering only the molecular ring, makes possible tuning of the transmission resonance shown in Fig. 4(a). Even in the absence of any applied gate voltage ($V_g = 0$), ZT vs temperature plotted in Fig. 4(c) is notably modified when compared to the corresponding functions in Fig. 2(d) for the two-terminal device. This stems from slight hybridization of the top gate and molecular states. The narrowing of the transmission peak around E_F due to the application of negative gate voltage enhances the thermopower in Fig. 4(b), thereby increasing ZT above its value at $V_g = 0$, which can be substantial at low temperatures as shown in Fig. 4(d).

In conclusion, we predict that a single conjugated molecule attached to metallic GNR electrodes, where the transparent molecule-GNR contact allows evanescent modes to penetrate from the electrodes into the HOMO-LUMO molecular gap generating a transmission resonance, can act as an efficient thermoelectric device. Our first-principles simulations suggest that its figure of merit can reach $ZT \sim 0.5$ at room temperature or $0.5 < ZT < 2.5$ below liquid nitrogen temperature, which is much higher than ZT found in other recent proposals for molecular thermoelectric devices.[8] The introduction of the third air-bridge top gate covering the molecule can change the sharpness of the resonance via the application of the gate voltage, thereby opening a path toward further optimization of ZT. We anticipate that much higher ZT could be achieved by *testing different types of molecules*[25] to reduce κ_{ph} because the power factor S^2G is already optimized in this class of devices based on ZGNR electrodes that generate molecular-level-independent transmission resonance, while the symmetry of propagating modes in ZGNRs lifts the compensation of hole-like and electron-like contributions to S.

We thank K. Esfarjani for illuminating discussions. Financial support under NSF Grant No. ECCS 0725566 (K.K.S. and B.K.N.) and FTP Grant No. 274-08-0408 (T.M. and K.S.T.) is gratefully acknowledged. The supercomputing time was provided in part by the NSF through TeraGrid resource TACC Ranger under Grant No. TG-DMR100002. K.K.S. and B.K.N. thank CAMD at the Technical University of Denmark for their kind hospitality while part of this work was being done.

*bnikolic@udel.edu

[1] C. B. Vining, Nat. Mater. **8**, 83 (2009).
[2] G. J. Snyder and E. S. Toberer, Nat. Mater. **7**, 105 (2008).
[3] A. J. Minnich *et al.*, Energy Environ. Sci. **2**, 466 (2009).
[4] P. Reddy *et al.*, Science **315**, 1568 (2007).
[5] Y. Dubi and M. Di Ventra, Rev. Mod. Phys. **83**, 131 (2011).
[6] M. Paulsson and S. Datta, Phys. Rev. B **67**, 241403(R) (2003).
[7] F. Pauly, J. K. Viljas, and J. C. Cuevas, Phys. Rev. B **78**, 035315 (2008); S.-H. Ke *et al.*, Nano Lett. **9**, 1011 (2009); C. M. Finch, V. M. García-Suárez, and C. J. Lambert, Phys. Rev. B **79**, 033405 (2009).
[8] D. Nozaki *et al.*, Phys. Rev. B **81**, 235406 (2010).
[9] O. Entin-Wohlman, Y. Imry, and A. Aharony, Phys. Rev. B **82**, 115314 (2010).
[10] P. Murphy, S. Mukerjee, and J. Moore, Phys. Rev. B **78**, 161406(R) (2008).
[11] T. Markussen, A.-P. Jauho, and M. Brandbyge, Phys. Rev. Lett. **103**, 055502 (2009).
[12] *Introducing Molecular Electronics*, edited by G. Cuniberti, G. Fagas, and K. Richter (Springer, Berlin, 2005).
[13] D. A. Areshkin and B. K. Nikolić, Phys. Rev. B **81**, 155450 (2010).
[14] K. K. Saha *et al.*, J. Chem. Phys. **131**, 164105 (2009).
[15] K. K. Saha *et al.*, Phys. Rev. Lett. **105**, 236803 (2010).
[16] S.-H. Ke, H. U. Baranger, and W. Yang, Phys. Rev. Lett. **99**, 146802 (2007).
[17] Y. M. Zuev, W. Chang, and P. Kim, Phys. Rev. Lett. **102**, 096807 (2009).
[18] J. Cai *et al.*, Nature (London) **466**, 470 (2010).
[19] O. V. Yazyev and M. I. Katsnelson, Phys. Rev. Lett. **100**, 047209 (2008).
[20] X. Guo *et al.*, Science **311**, 356 (2006).
[21] T. Markussen, R. Stadler, and K. S. Thygesen, Nano Lett. **10**, 4260 (2010).
[22] J. P. Bergfield and C. A. Stafford, Nano Lett. **9**, 3072 (2009).
[23] K. Esfarjani, M. Zebarjadi, and Y. Kawazoe, Phys. Rev. B **73**, 085406 (2006).
[24] J. Enkovaara *et al.*, J. Phys. Condens. Matter **22**, 253202 (2010).
[25] See Supplemental Material at http://link.aps.org/supplemental/10.1103/PhysRevB.84.041412.